CTU Journal of Innovation and Sustainable Development
ISSN 2588-1418 | e-ISSN 2815-6412

DOI:10.22144/ctujoisd.2024.313

Integrating the cellular vortex method with remote sensing and geographical information systems in the modelling of coastal flooding around Niger Delta

Mokwenye-Ikebu Ifesinachi, Ihimekpen Ngozi Isioma, Okonofua Ehizonomhen Solomon, and Ilaboya Idowu Rudolph*

Department of Civil Engineering, Faculty of Engineering, University of Benin, Nigeria

**Corresponding author (rudolph.ilaboya@uniben.edu)*

Article info.

Received 23 Jan 2024
Revised 25 Mar 2024
Accepted 15 Jun 2024

Keywords

Cellular vortex element, flood modelling, geographical information system, natural disaster and remote sensing

ABSTRACT

Coastal areas are increasingly vulnerable to flooding, necessitating accurate simulation methods to understand flood dynamics and their potential impacts. This study employed a Lagrangian framework integrating the cellular vortex method with remote sensing and GIS to simulate flood height distribution in a coastal region. Leveraging climatic and remotely sensed data, alongside ArcMap 10.6.1 for map processing, the research estimated flood magnitude and frequency using the L-moment approach, applied to a forty-year tidal record dataset. Essential input parameters, such as the roughness coefficient and curve number, were derived from land use and land cover characteristics. Additionally, river flow velocity was observed at 0.12m/s, with measured wind speed and direction recorded at 4m/s in the northwest direction. Notably, analysis of the initial flood height distribution map revealed a significant expansion of wetland areas, attributed to observed land use changes between May 2002 and July 2005. Projections for flood height distribution in 2025 and 2050 highlighted the emergence of tidal floods, emphasizing the critical role of considering future climate and land use scenarios in flood dynamics assessment. This research contributes to advancing understanding of flood modeling techniques and underscores the urgency of adaptive measures to mitigate the potential impacts of coastal flooding.

1. INTRODUCTION

The severity and frequency of natural disasters have increased significantly over time due to various contributing factors (Han et al., 2020). This escalation, accelerated by physical forces and human activities, poses substantial threats to ecosystems and the environment on a large scale (Ali et al., 2019). Floods are one of the most common and destructive hydro-meteorological disasters, presenting substantial threats to social, economic, and environmental aspects of human life (Ritter et al., 2020). From 1996 to 2015, there were about 150,061 flood incidents worldwide, contributing to 11.1% of disaster-related deaths globally, as reported by the United Nations Office for Disaster Risk Reduction (UNISDR) (Hong et al., 2018; Wei et al., 2019). Floods not only cause immediate economic damage and loss of human life but also trigger long-term secondary effects, including disease outbreaks and malnutrition in affected communities (Cao et al., 2016; Tomczyk et al., 2020). Recent years have witnessed a significant increase in the frequency and severity of floods worldwide (Alho et al., 2008; Klijn, 2009). This surge in flooding incidents is often attributed to ongoing climate change, driven by greenhouse gas emissions and exacerbated by changes in land use

patterns resulting from human activities, extreme weather events, and hydro-meteorological phenomena (Fohrer et al., 2001; Sofia et al., 2017; Kundzewicz et al., 2018; Aja et al., 2019). Floods are characterized by the overflow of water onto land, leading to partial or complete inundation of normally dry areas (Ehiorobo et al., 2012; Izinyon, 2018). The voids in the soil become filled with water, exceeding the soil's infiltration capacity and resulting in surface runoff. Coastal cities, such as those in the Niger Delta, are particularly vulnerable to flooding due to their low-lying nature and proximity to water bodies (Lichter et al., 2010). Despite this vulnerability, there is a lack of comprehensive flood information and inadequate attention to flood modeling and vulnerability assessment in Nigeria compared to other developing countries (Kun et al., 2014; Nkwunonwo et al., 2015). Traditional methods for simulating flood events rely on hydraulic and hydrological approaches, which often require extensive data inputs and neglect certain physical terms, especially in unsteady flows (Zeynab et al., 2018; Suyeon et al., 2018). However, the cellular vortex element method has emerged as a promising alternative for analyzing complex and unsteady flows, including coastal flooding scenarios (Viganò & Maddalena, 2018). This numerical method, based on simple physics principles, offers accurate solutions to engineering challenges, such as coastal flooding, without the complexity and computational burden associated with conventional turbulence models.

This study aim to address this research gap by focusing on simulating flood height distribution in a coastal area using a Lagrangian framework integrated with the cellular vortex method, remote sensing, and GIS. The objectives include estimating flood magnitude and frequency, deriving essential input parameters from land use and land cover characteristics, and analyzing the impact of future climate and land use scenarios on flood dynamics. By employing advanced modeling techniques and spatial data analysis methods, this research seeks to provide valuable insights into flood dynamics in coastal areas, ultimately contributing to enhanced flood management strategies and adaptation measures.

2. MATERIALS AND METHODS

2.1. Study area

The study area is Ugborodo clan. Ugborodo is a riverine rural community, situated between the Atlantic Ocean on the west and Escravos River on the south. Ugborodo is the headquarters of Ugborodo Clan of the Itsekiri ethnic group. The town lies between longitude E5.10-5.15^0 and Latitude N5.4-5.65^0. The area's climate is characterized as wet equatorial, influenced by its proximity to the equator and the Gulf of Guinea. There are two distinct seasons: the rainy season, which typically runs from April to October, and the dry season, from November to March. The rainy season has two peak periods, from May to July and from August to October, with the heaviest rainfall occurring during the second peak, often resulting in flooding across the community. Ugborodo is an island boarded with distinct coastal settlements at the Northern part by Okiomekpo, and Ogidigben at the South-Eastern flank. It is rich in aquatic life which has attracted many people from other states of the country and beyond like the Ilaye's, Ghanians and Cameroonians who are involved in fishing activities for their livelihood and with others involved in farming, lumbering, craft work, trading, palm oil making, etc. Ugborodo clan is predominantly a Christian community but few of its indigenes still worship the goddess of the sea called Umalokun and have a present population of about 177,000 and a very large expanse of land. The map of the study area is presented in Figure 1.

Figure 1 Study area map

2.2. Data requirement/acquisition

Both remotely sensed data and field data were utilized for the study, with detailed information including scale, source/date, and type presented in Table 1.

Table 1. List of data employed for the study

S/n	Data / Scale	Type	Source /Date
1	Landsat 8 Satellite imagery (30m Resolution)	Remotely sensed	USGS (2018)
2	SRTM Data (10m DEM Resolution)	Remotely sensed	USGS (2018)
3	Topographical map 1:100,000	Digital Copy	Federal Survey (2018)
4	Geological Map (1:500,000)	Digital copy	Nigerian Geological survey Agency(2018)
5	FAO Soil Data	Remotely Sensed	FAO (2018)
6	Rainfall Data	40 years Annual Data	1978–2018
7	Discharge Data	Annual Peak Discharge Data	1978–2018

The topographical map and geological map were sourced from the Office of the Surveyor General of the Federation and the Nigerian Geological Survey Agency, respectively. Discharge data were retrieved from historical records gathered using hydromet instruments. Remotely sensed data were downloaded from their respective websites. Following acquisition, all data underwent processing using PCI Geomatica v16 and ArcMap 10.6.1.

2.3. Satellite data processing

All satellite images acquired were first projected onto the Universal Transverse Mercator (UTM) coordinate system using the WGS84 UTM32N datum. Similarly, all hard copy maps were scanned and then geo-referenced to align with the same UTM coordinate system (WGS84 UTM32N). Following this, a defined boundary extent, referred to as the 'Area of Interest', was established. All acquired data, including satellite images and scanned maps, were clipped to this specified 'Area of Interest' using the Clip tool within the ArcMap environment. Subsequently, drainage and elevation maps were generated utilizing a digital elevation model (DEM). Geological and topographical maps were created through the digitization of geological

unit's characteristic to the study area, along with relevant settlement and geographical features.

2.4. Estimation of flood return periods

The estimation of flood occurrence magnitude and frequency across various return periods (2, 5, 10, 25, 50, 100, and 200 years) in the Escravos River involved applying the L-moment approach to a forty-year tidal record dataset. Annual peak discharge values from the Escravos tidal gauge spanning fifteen years (2000 to 2014) were utilized, while the remaining twenty-five years of runoff data were simulated using the intensity duration frequency (IDF) approach. The simulated data was validated against the tidal gauge records. The rainfall intensities corresponding to the specified return periods were determined using the IDF approach.

$$K_T = -\frac{\sqrt{6}}{\pi}\left\langle 0.5772 + \ln\left[\ln\left(\frac{T}{T-1}\right)\right]\right\rangle \quad (1)$$

Where **T** represents the chosen return period. The rainfall intensity for a given return period was calculated using the following formula:

$$X_T = \bar{X} + K_T \sigma \quad (2)$$

Where X_T; is the rainfall intensity corresponding to a specified return period T (yrs), $\bar{X}$; is the mean rainfall intensities and σ ; is the standard deviation of rainfall intensities. Using the computed rainfall intensity, and adopting the rational formula the runoff discharge was computed as;

$$Q = 0.028(p * A * I_c \quad (3)$$

Where;

Q is the runoff discharge (m^3/s), A is the catchment area (m^2), I_c is intensity of rainfall per hour and P is the coefficient of runoff which is dependent on the soil type.

2.5. Determination of roughness coefficient

The roughness coefficient, a crucial input parameter for the cellular vortex technique, was obtained from Manning's roughness coefficient reference table, as presented in Table 2. This reference table was developed specifically based on land use and land cover classification

Table 2. Manning's roughness coefficient based on LULC (Amna et al., 2015)

Anderson Code	Description	Manning Roughness
100	Urban and Built-up Land	0.03
211	Dryland, Cropland and Pasture	0.03
212	Irrigated Cropland and Pasture	0.035
213	Mixed Dryland/Irrigated Cropland and Pasture	0.033
280	Cropland/Grassland Mosaic	0.035
290	Cropland/Woodland Mosaic	0.04
311	Grassland	0.05
321	Scrubland	0.05
330	Mixed scrubland/Grassland	0.05
332	Savanna	0.06
411	Deciduous Broadleaf Forest	0.1
412	Deciduous Needleleaf Forest	0.1
421	Evergreen Broadleaf Forest	0.12
422	Evergreen Needleleaf Forest	0.12
430	Mixed Forest	0.1
500	Water Bodies	0.035
620	Herbaceous Wetland	0.05
610	Wooded Wetland	0.05
770	Barren or Sparsely Vegetated	0.03
>800	Tundra. Snow or Ice	0.05

2.6. Curve number (CN) determination

In determining the curve number (CN) for the study area, various factors were taken into account, including the hydrologic soil group (HSG), land cover type, treatment practices, hydrologic condition, and antecedent runoff condition (ARC). The CN value was derived by consulting a table that correlates hydrologic soil groups with vegetation types. Table 3 was specifically used to characterize the area, aiding in the selection of the most suitable curve number.

Table 3. Runoff curve numbers for urban areas (The World Bank, 2009)

---- Cover description ---- Cover type and hydrologic condition	Average percent Impervious area	Curve numbers for -- hydrologic soil group --			
Fully developed areas (vegetation established)		A	B	C	D
Open space (lawns, parks, golf courses, cemeteries)					
Poor condition (grass cover < 50%)		68	79	86	89
Fair condition (grass cover 50% to 75%)		49	69	79	84
Good condition (grass cover >75%)		39	61	74	80
Impervious areas: Paved parking lots, roofs, driveways, etc.					
(excluding right-of-way)		98	98	98	98
Streets and roads					
Paved; curbs and storm sewers (excluding right-of-way)		98	98	98	98
Paved; open ditches (including right-of-way)		83	89	92	93
Gravel (including right-of-way)		76	85	89	91
Dirt (including right-of-way)		72	82	87	89
Western desert urban areas					
Natural desert landscaping (pervious areas only)		63	77	85	88
Artificial desert landscaping (impervious weed barrier, desert shrub with 1-to 2- inch sand or gravel mulch and basin borders)		96	96	96	96
Urban districts					
Commercial and business	85	89	92	94	95
Industrial	72	81	88	91	93
Residential districts by average lot size:					
1/8 acre or less (town houses)	65	77	85	90	92
1/4 acre	38	61	75	83	87
1/3 acre	30	57	72	81	86
1/2 acre	25	54	70	80	85
1 acre	20	51	68	79	84
2 acres	12	46	65	77	82
Newly graded areas					
pervious areas only, no vegetation		77	86	91	94

2.7. Flood modelling using cellular vortex technique

The cellular vortex method was used to perform numerical simulations of flooding in the coastal catchment area of Ugborodo clan, which was chosen for its importance in fluid dynamics and its ability to accurately depict vorticity dynamics. This method involves tracking vorticity evolution through vortex particles, offering a robust solution to fluid flow problems. To comprehensively analyze flood patterns and their future impacts on Ugborodo clan, various parameters were integrated into the main model. These parameters include flood discharge for return periods of 2, 5, 10, 25, 50, 100, and 200 years, wind velocity and direction data obtained with a multi-parameter handheld anemometer, and Manning's surface roughness factor derived from relationships between surface characteristics, soil type, and land use/land cover. The primary objective of the vortex element model was to delineate the study area, generate flood inundation maps, and evaluate susceptibility to flood hazards across different return periods. The model development was based on several key assumptions:

1. Only critical parameters affecting flooding and surface water flow—such as discharge, land use, and soil type—were considered;
2. The Escravos River, which originates from the River Niger and drains into the Atlantic Ocean, was divided into two sections: reach 1 (2.2 km downstream from the Escravos River) and reach 2 (2.2 km downstream from the Bight of Guinea through the Atlantic Ocean). Both sections were identified as significant contributors to flooding;

3. The primary sources of flooding in the study area were assumed to be the Escravos River and the River Niger;
4. Vegetation cover was considered to have a negligible effect on rainfall interception due to the area's land use and land cover characteristics;
5. Infiltration and percolation rates were modeled based on total water percolation, with zero infiltration and percolation assumed due to the saturated soil conditions

The input requirement needed for the cellular vortex element method and the corresponding values are presented in Table 4.

The flowchart for coastal flood simulation using the cellular vortex technique is presented in Figure 2.

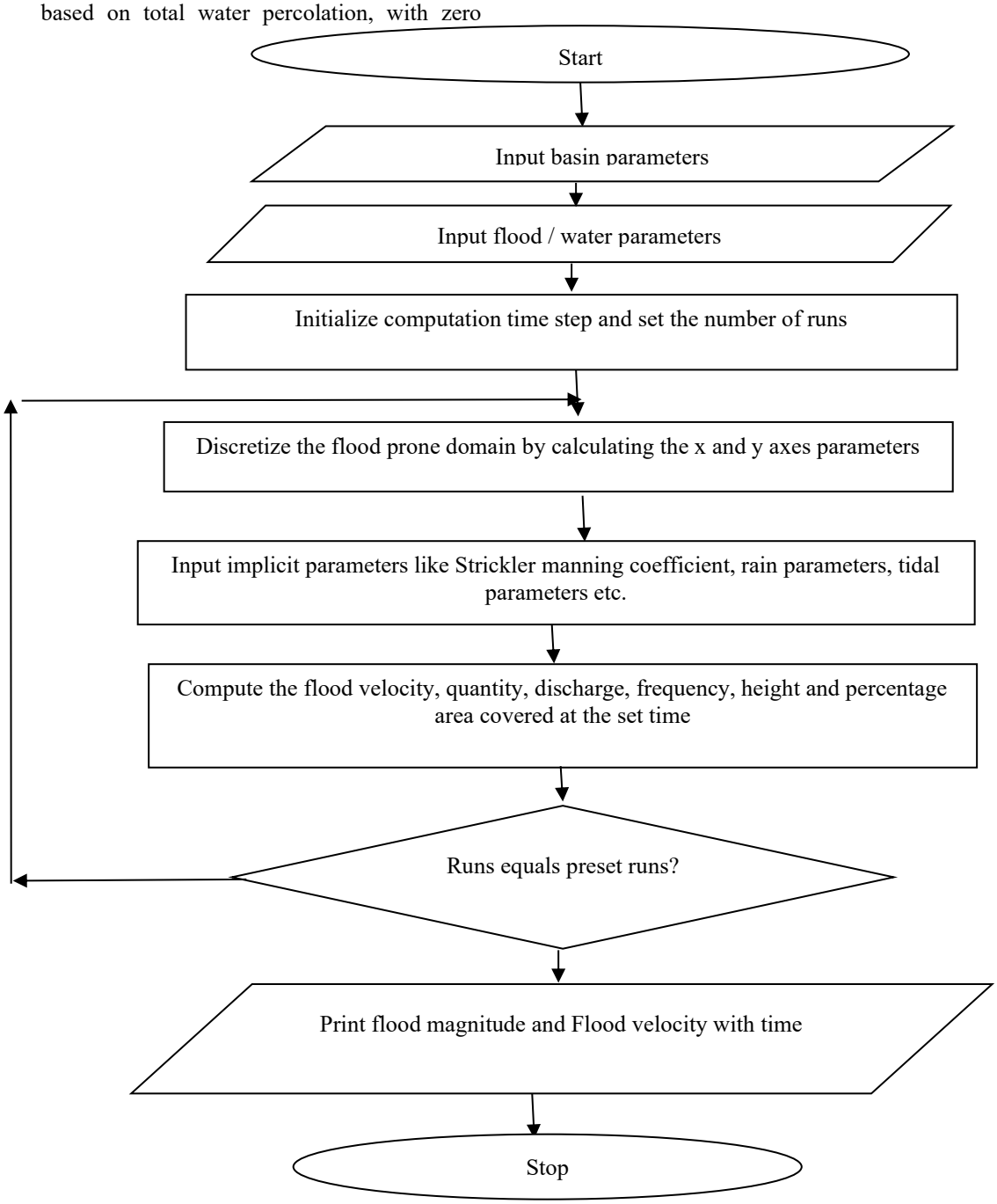

Figure 2. Flowchart for coastal flood simulation using cellular vortex method

Table 4. Data requirement/acquisition for flood simulation

Required Input Data	Mode of Acquisition/Result
Flood discharge for 2yrs, 5yrs, 10yrs, 25yrs, 50yrs 100yrs and 200yrs return period	Flood magnitude for the selected return period was acquired by L-Moment Approach
Wind velocity/direction	Hand-held Ananometer was used to determine the speed and direction of wind; the result gave a maximum wind speed of 4m/s in the N-W direction
Manning's surface roughness factor	Land use Land cover map was developed and classified. Then, the relationship between surface roughness and land use was employed to select the manning constant value. For mixed dry land/Irrigated cropland, a constant of 0.033 was adopted. For urban and built-up area, a constant of 0.03 was used while 0.017 was adopted for shore area.
Rainfall intensity	Rainfall intensities were estimated using intensity duration frequency approach
River flow velocity	Determined with the aid of a flow meter and was observed to be 0.12m/s
Area of simulation surface (Length/Width)	2,200
Grid lines division x/y direction	10

3. RESULTS AND DISCUSSION

3.1. Thematic maps of flood inducing factors

Flood-inducing factors refer to the various factors that can influence or contribute to flooding. These factors are crucial in understanding and predicting flood events. Using the DEM, the elevation map of the study area was developed and presented in Figure 3.

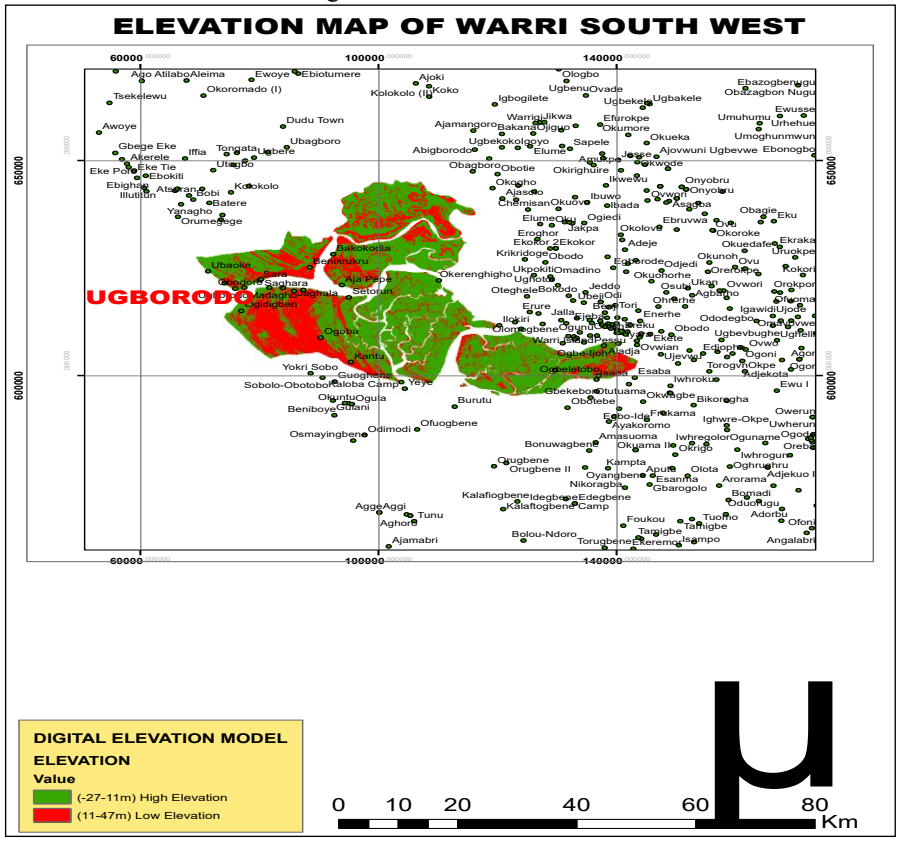

Figure 3. Elevation map of the study area

From the map of Figure 3, it was observed that the study area Ugborodo community lies within the low elevation region. Low-lying areas with elevations close to or below sea level are particularly susceptible to coastal and tidal flooding. During storm surges, high tides, or heavy rainfall, water can inundate these areas, leading to widespread flooding (Chen & Liu 2014). To get an insight into the rainfall distribution around the study area, the precipitation map of the study area was developed and presented in Figure 4.

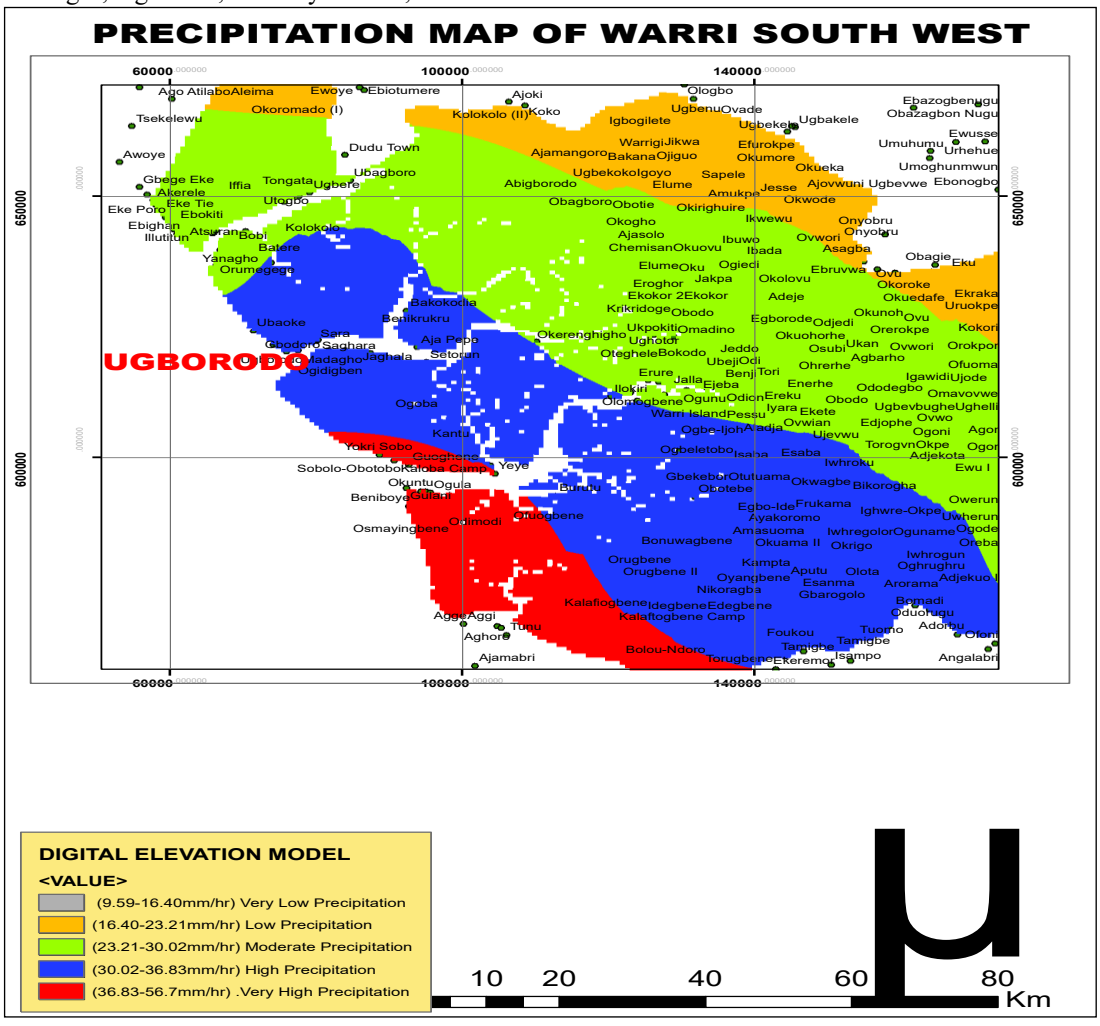

Figure 4. Precipitation map of the study area

The map in Figure 4 indicates that Ugborodo community falls within a region of heavy precipitation. Precipitation, which includes rain, snow, sleet, and hail, is a major factor contributing to floods. It is central to many flood events and can cause different types of flooding. Rainfall, in particular, affects flooding based on its volume, intensity, and duration. Prolonged and intense rainfall can result in surface water flooding, also referred to as pluvial flooding. This occurs when the rainfall rate surpasses the land's or urban infrastructure's drainage capacity, leading to water pooling on the surface, flooding streets, properties, and low-lying areas (Sarkar & Mondal 2020).

To understand the rate of water infiltration around the study area, the soil map was generated and presented in Figure 5.

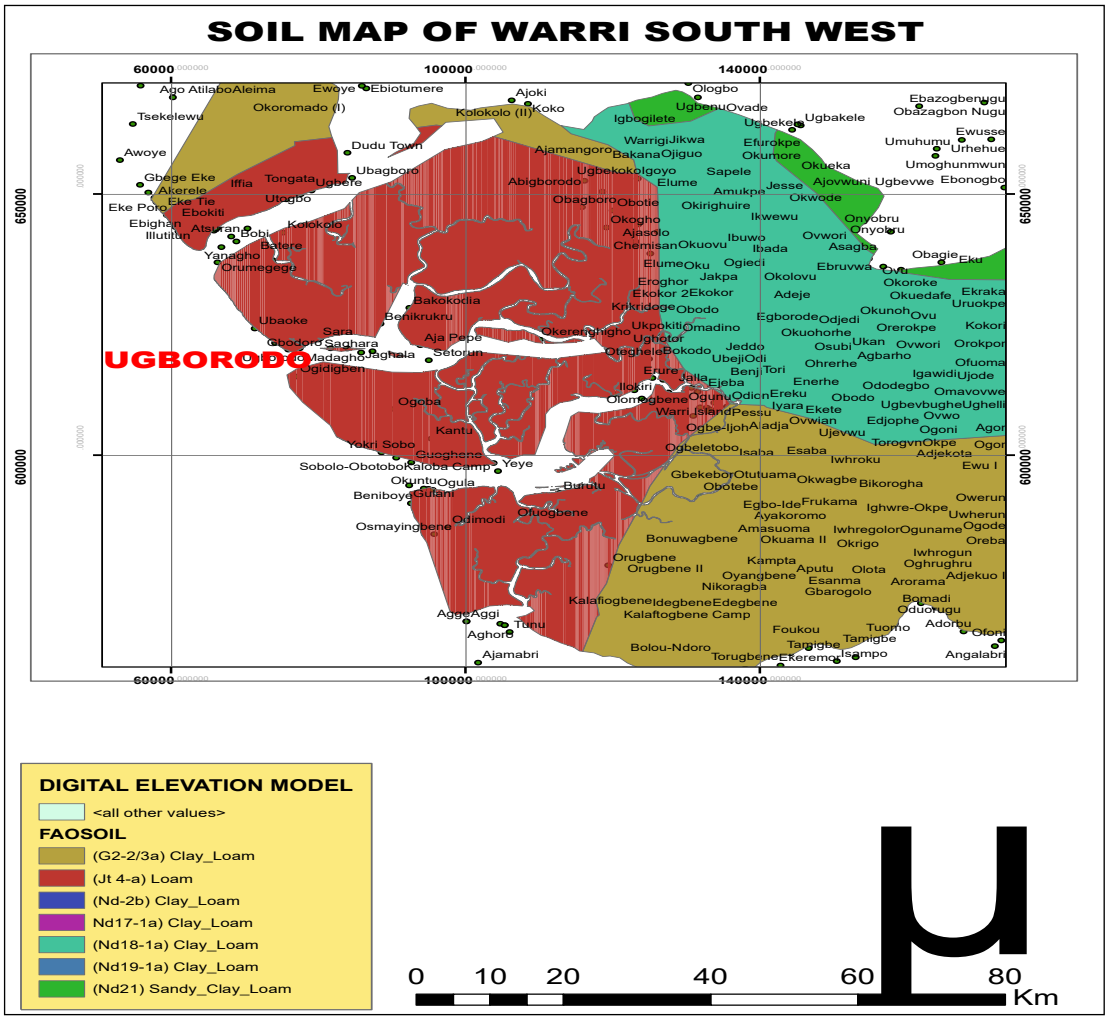

Figure 5. Soil map of the study area

From the map of Figure 5, it was observed that the soil around the study area Ugborodo community is defined by clay- loamy characteristics. Soil can have a significant contribution to flooding in various ways, primarily by affecting how water is absorbed, retained, or rapidly transported across the landscape. When the voids in soil are filled with water, it invariably means that the infiltration capacity of the soil has been exceeded. Then, the remaining water flows on the surface as runoff and runoff, if not well managed, can cause flood. For clay-loamy soil which characterizes the study area, the infiltration capacity quickly exceeded as the intensity of rainfall increases owing to the impermeable nature of clay soil.

The drainage density of the study area was also developed and presented in Figure 6.

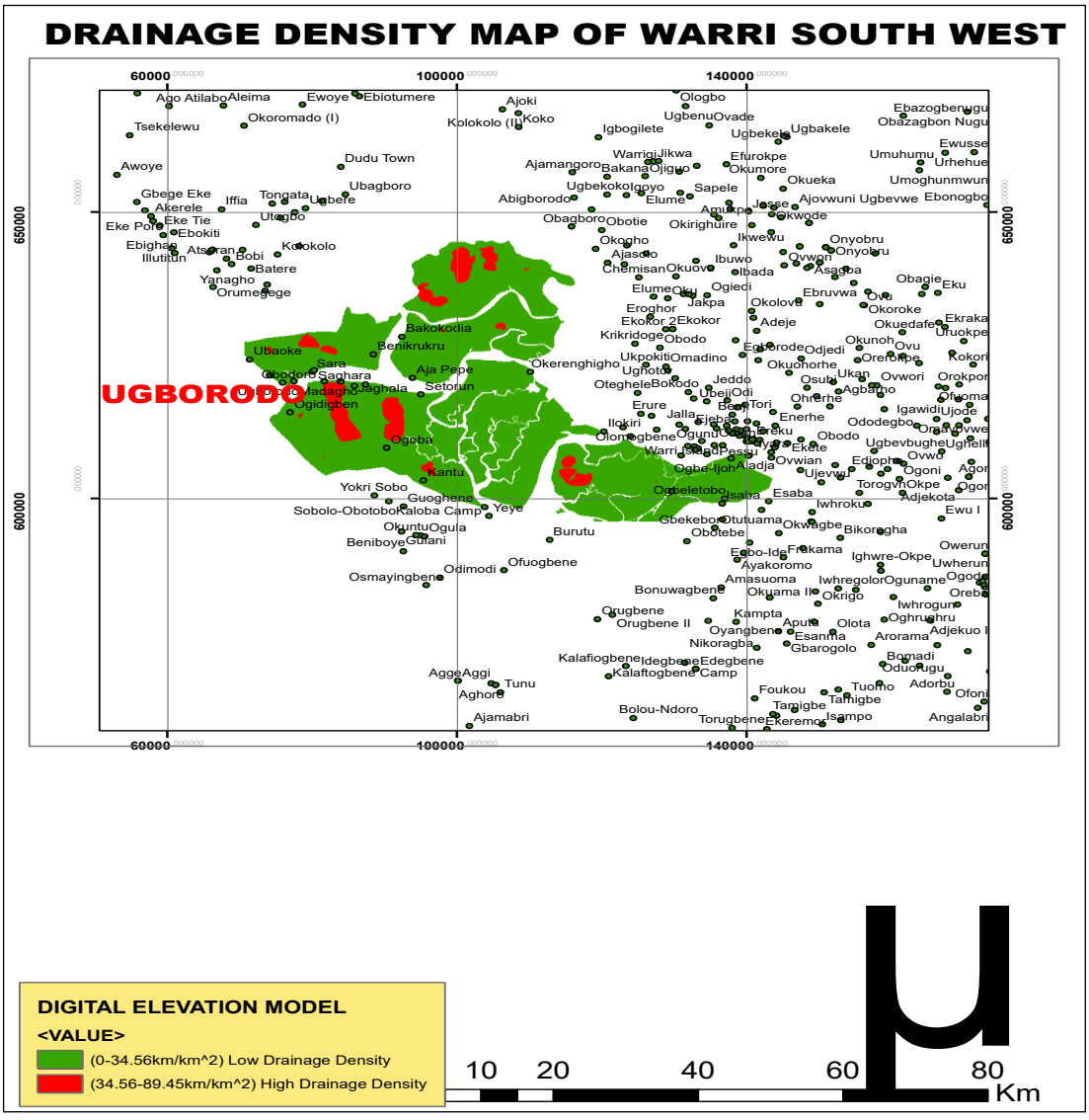

Figure 6. Drainage density map of the study area

As observed in Figure 6, the study area lies within a low drainage density region. By implication, there may not be enough natural drainage pathways to carry the runoff water from the soil. Drainage density is a key factor in understanding and predicting flooding, particularly in regions with complex hydrological systems. It refers to the concentration of streams, rivers, and watercourses within a given area. The classification of land use around the study area from the period 2013 to 2018 is presented in Figure 7.

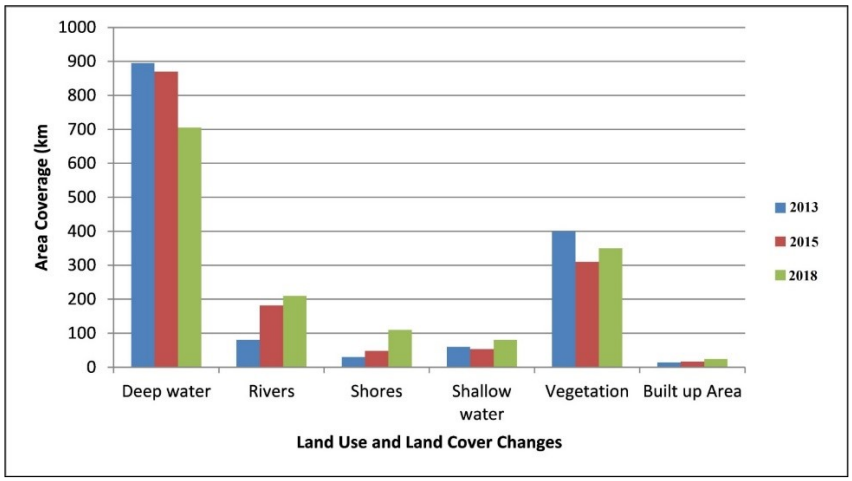

Figure 7. Temporal pattern of land use/cover changes around the study area

A classification scheme was created by integrating data from satellite imagery with existing knowledge of the study area. Six land use classes were identified within the study area using a supervised classifier algorithm for satellite image classification. In 2013, the deep-water body coverage was at its highest, measuring 895 km², while in 2018, it recorded the lowest coverage at 703 km². The vegetation covers also had the highest coverage of 400 km^2 in 2013, and the lowest coverage was in 2015 with the value of 310 km^2. The built-up areas gradually increased from 2013 to 2018 from 14 km^2 to 24 km^2. The shores also increased from 30 to 110 km^2 for the period of study which indicates that the shore line is retreating. As population density rises in coastal areas, coastal erosion emerges as a significant issue along many of Nigeria's coastal margins. The land use and land cover (LULC) in these regions are crucial factors concerning flood risk and coastal flooding.

3.2. Estimation of rainfall intensity

Rainfall intensity is defined as the ratio of the total rainfall depth that occurs over a specific period to the duration of that period, typically expressed in units such as millimeters per hour (mm/h). For the study area, rainfall intensity was calculated and used to construct the intensity-duration-frequency (IDF) curve, which is displayed in Figure 8. This curve provides insight into the relationship between rainfall intensity, duration, and frequency, which is essential for understanding the region's potential for flood events and designing effective flood management strategies.

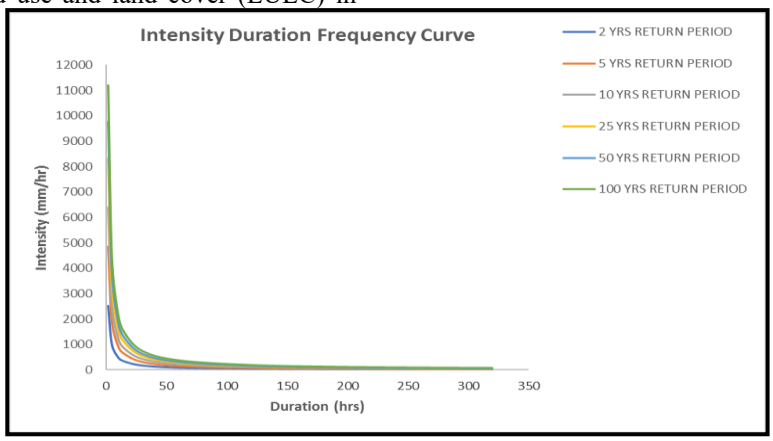

Figure 8. IDF curve based on Gumbel distribution

For a square area of 5000 m^2, with rainfall duration of 0.25 hrs and runoff coefficient of 0.53, the runoff discharge around the study area was simulated using the rational formula and the time series plot of estimated runoff against time is presented in Figure 9.

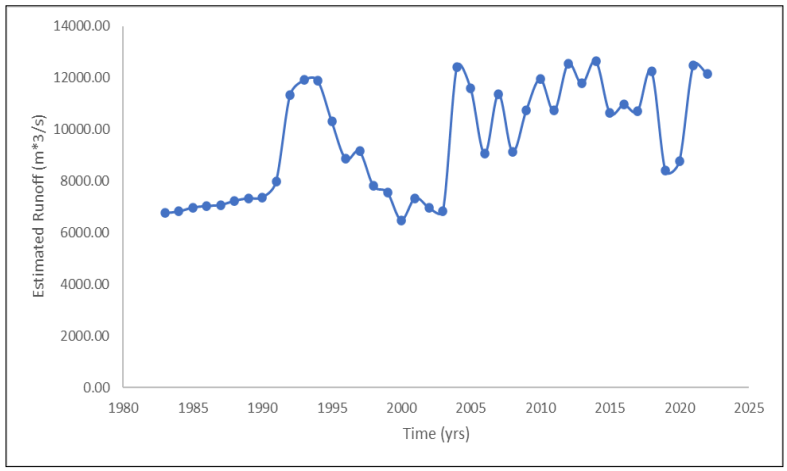

Figure 9. Time series plot of runoff in the study area

L-moment computation was conducted using runoff data. In the analysis, three probability distribution models were utilized: generalized extreme value, generalized Pareto, and generalized logistic distribution. The most suitable model among the candidate distributions fitted to the observed data was chosen by applying five statistical goodness-of-fit tests to their predicted values: Root Mean Square Error (RMSE), Relative Root Mean Square Error (RRMSE), Maximum Absolute Deviation Index (MADI), Maximum Absolute Error (MAE), and Probability Plot Correlation Coefficient (PPCC).

The overall goodness of fit for each distribution was assessed using a ranking scheme that compared three categories of test criteria based on the relative values of the statistical test results. The Generalized Extreme Value (GEV) probability distribution received the highest total score of 15 and was therefore selected as the best probability distribution model for predicting runoff at various return periods. The results are presented in Table 5.

Table 5. Estimated runoff magnitude at different return period

Return Periods (T)	Estimated Runoff Magnitude (m^3/s)
2yrs	12107.06930
5yrs	12877.70461
10yrs	13269.48809
25yrs	13660.83651
50yrs	13891.31459
100yrs	14079.59222
200yrs	14397.27163

3.3. Food simulation using voltex element method

Inverse distance weighting method was used for the geospatial interpretation of the flood raster. Based on the interpretation, the geomorphological features of the floodplain were classified into; dry land, wet land, flash flood, combination of flash and river flood and tidal flood. The raster layers were thereafter reclassified into five classes using an equal interval and the classified flood heights were assigned the following values and colour for the graphical user's interface.

1. 0.0000-1.4500 (Dry Land): Dark Green
2. 1.4600-1.6500 (Wet Land): Light Green
3. 1.6600-1.7500 (Flash Flood): Yellow
4. 1.7600-1.8500 (Flash + River Flood): Brown
5. 1.8600> Tidal Flood Red

Two different sets of simulation were done using the cellular vortex element method and they include;

1. Initialization: this initial simulation was done to ascertain the previous flood situation in the study area and was done for the years 2002, 2005, and 2010. For each year the simulation was done for the months of February, May, July, September, November and December in order to capture the impact of seasonal variability.
2. Predictive: this simulation was done to predict the future flood situation in the study area and was done for the years 2025 and 2050 covering the months of February, May, July, September, November and December for each predicted year.

Results of initialization are presented in Figures 10 and 11 representing May 2002 and July 2005 while the predictive simulation is presented in Figures 12 and 13 representing May 2025 and July 2050, respectively.

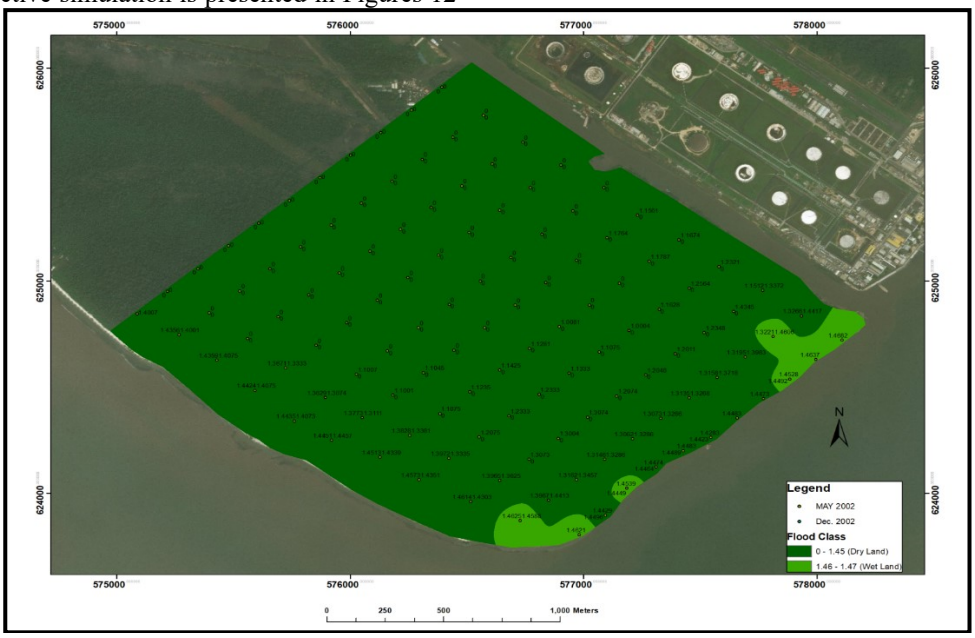

Figure 10. Flood height distribution for May 2002

The appearance of light green colouration, as observed in Figure 10, signifies wet land. The flood height around this region usually ranged from 1.4600 m to 1.6500 m. The increased flood height in this region can be attributed to the low drainage density that characterizes the study area. It was also observed that the area covered by wet land is small, as observed in Figure 10. This can be attributed to the low rainfall intensity usually experienced in the months of May. As we progress into July, the intensity of rainfall increases and the area of wet land was seen to have increased as observed in Figure 11.

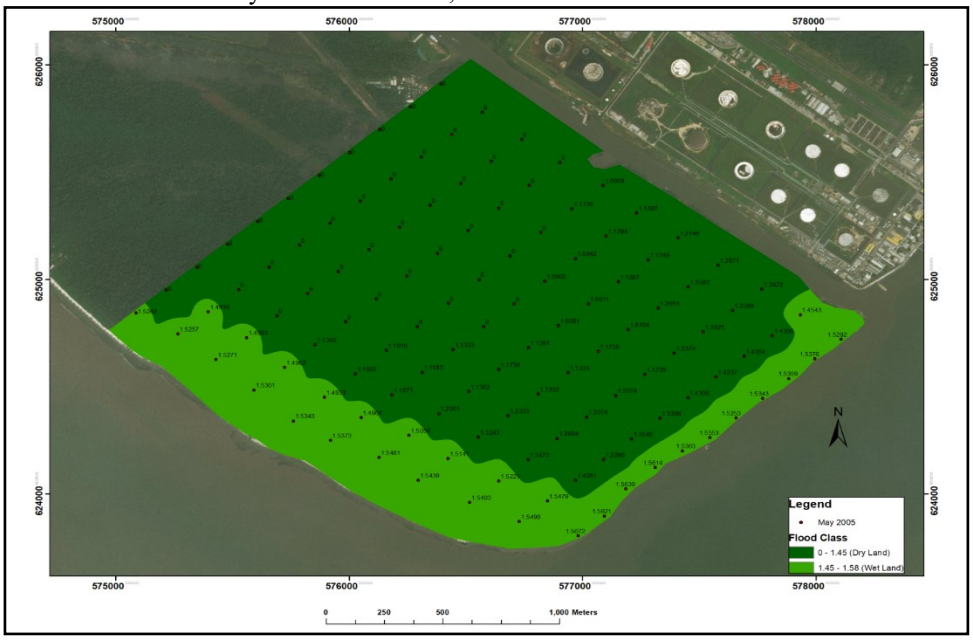

Figure 11. Flood height distribution for July 2005

From the flood height distribution map, it was observed that the area covered by wetland has increased considerably. The increased wetland area observed in July 2005 compared to May 2002 can be attributed to the land use change that occurred in the study area. It was observed that the built-up area gradually increased from 14 km^2 in 2013 to 24 km^2 in 2018. The increase in built-up area resulted in a decrease in the rate of infiltration and percolation, which consequently led to an increased runoff rate. The predicted flood height distribution for May 2025 and July 2050 is presented in Figures 12 and 13, respectively.

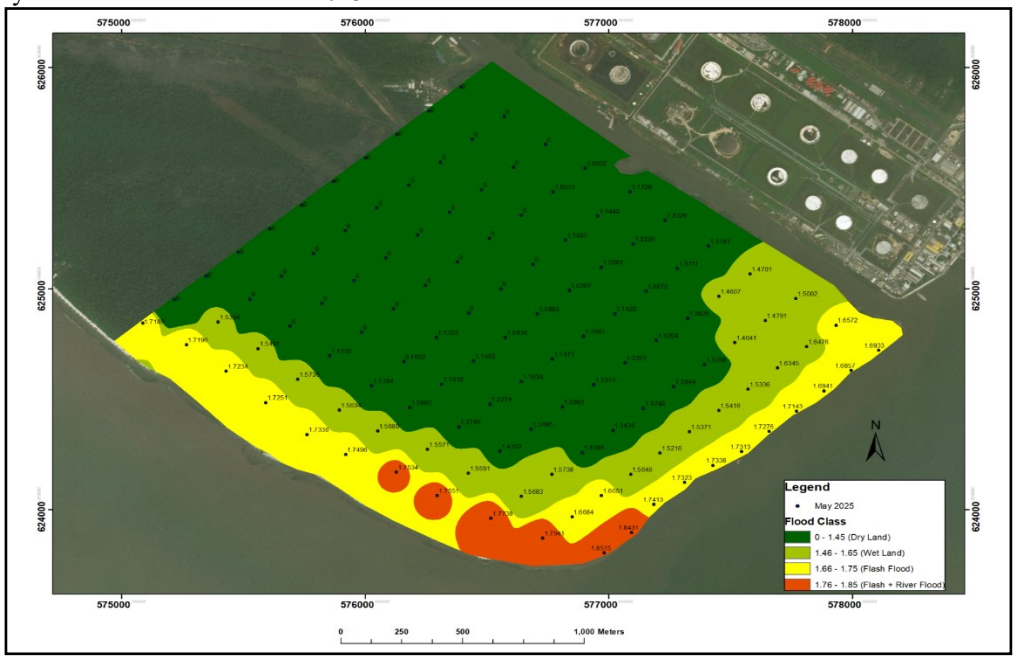

Figure 12. Predicted flood height distribution for May 2025

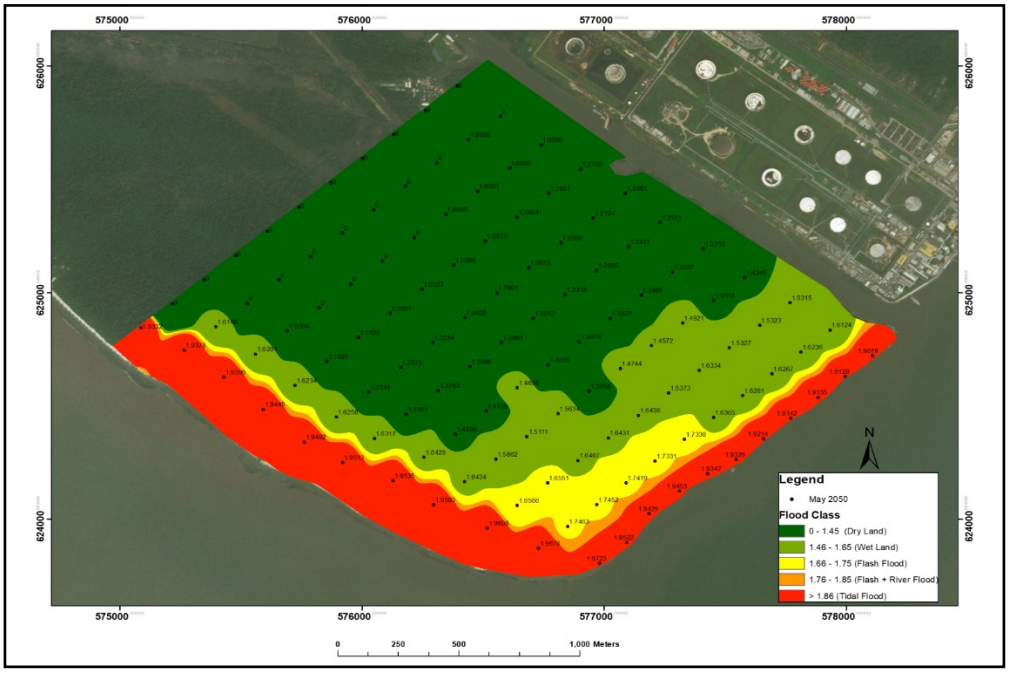

Figure 13. Predicted flood height distribution for May 2050

The flood height distribution map of Figure 12 shows four distinct colours, namely green, light green, yellow, and brown, representing dry land, wetland, flash flood and flash flood plus river flood. By 2050, there is the appearance of red colour, as observed in Figure 13, which represent tidal flood. The vortex element method of flood prediction was able to use the predicted return period data, land use surface roughness and the prevailing environmental condition of the study area to predict the flood height distribution for the years 2025 and 2050.

4. CONCLUSIONS

This study employed the cellular vortex element method to simulate floods in the Niger Delta region of Nigeria. The analysis demonstrated the method's efficacy in examining coastal flooding, as it considers the acceleration, convective, and diffusive characteristics of fluid particles. Additionally, the hydraulic characteristics of the study area revealed its low-lying terrain with low drainage density. The predictive flood simulation results indicated the development of wetlands, flash floods, river floods, and tidal floods resulting from gradual changes in precipitation and land use/land cover. These findings carry significant implications for flood management and disaster preparedness in the region. Early warning systems developed from the research results can be crucial in mitigating the impacts on lives and properties in vulnerable communities, pending government approval for sea wall construction. Additionally, identifying areas at risk for various types of floods offers valuable insights for targeted intervention and adaptation strategies. Looking to the future, planning should emphasize the implementation of adaptive measures, such as constructing sea walls and improving drainage systems, to enhance resilience against flood hazards. Ongoing monitoring and research efforts are vital for refining predictive models and gaining a deeper understanding of the evolving dynamics of coastal flooding in light of climate change and urbanization. The validation of the research findings against the 2015 tidal report from the Nigerian Navy demonstrated strong agreement, thereby increasing confidence in the study's outcomes. Overall, this study contributes to advancing knowledge and informing decision-making processes aimed at reducing the vulnerability of coastal communities to flood disasters in the Niger Delta region.

REFERENCES

Aja, D., Elias, E., & Obiahu, O. H. (2019). Flood risk zone mapping using rational model in a highly weathered Nitisols of Abakaliki Local Government Area South-eastern Nigeria. *Geology*, *Ecology*, *and Landscape*, *4*(2), 131–139.

Alho, P., Sane, M., Huokuna, M., Käyhkö, J., Lotsari, E., & Lehtiö, L. (2008). Mapping of floods. *Environmental Administration Guidelines*, *2*, 59-101.

Ali, S. A., Khatami, R., Ahmad, A., & Ahmad, S. N. (2019). Application of GIS based analytic hierarchy process and frequency ratio model to flood vulnerable mapping and risk area estimation at Sundarban region India. *Model Earth Systems and Environment*, *5*(3), 1083–1102.

Cao, C., Xu, P., Wang, Y., Chen, J., Zheng, L., & Niu, C. (2016). Flash flood hazard susceptibility mapping using frequency ratio and statistical index methods in coalmine subsidence areas. *Sustainability*, *8*, 948.

Chen, W. B., & Liu, W. C. (2014). Artificial neural network modeling of dissolved oxygen in reservoir. *Environmental Monitoring and Assessment*, *186*(11), 7469-7483.

Ehiorobo, J. O., Izinyon, O. C., & Ilaboya, I. R. (2012). *Effects of climate change on river flow regimes in the mangrove and tropical rain forest region of West Africa* [Conference presentation]. International Workshop on Exchange of Experience in Water Resources Management between Europe/China/Africa/Latin America.

Fohrer, N., Haverkamp, S., Eckhardt, K., & Frede, H. G. (2001). Hydrologic response to land use changes on the catchment scale. *Phys. Chem. Earth.*, *26*, *577–582.*

Han, Y., Huang, Q., He, C., Fang, Y., Wen, J., Gao, J., & Du, S. (2020). The growth mode of built-up land in floodplains and its impacts on flood vulnerability. *Science of the Total Environment*, *700*, 134462.

Hong, H., Panahi, M., Shirzadi, A., Ma, T., Liu, J., Zhu, A. X., Chen, W., Kougias, I., & Kazakis, N. (2018a). Flood susceptibility assessment in Hengfeng area using coupling adaptive neuro-fuzzy inference system with genetic algorithm and differential evolution. *Sci. Total Environ*, *621*, 1124–1141

Izinyon, O. C. (2018). *Flood hazard modelling and management* [Conference presentation]. The technical sections of the Nigeria Society of Engineers.

Klijn, F. (2009). *Flood risk assessment and flood risk management: An introduction and guidance based on experience and findings of FLOOD site* (an EU-funded Integrated Project). Delft: Deltares, Delft Hydraulics.

Kun, Y., Angelica, T., Gabor, B., Tommaso, M., & Di-Baldassarre, G. (2014). Exploring the potential of topography and radar altimetry to support flood

propagation modeling: Danube case study. *Journal of Hydrologic Engineering*, *20*(2), 04014048.

Kundzewicz, Z.W., Pinskwar, I., & Brakenridge, G. R. (2018). Large floods in Europe 1985–2009. *Hydrological Science Journal*, *58*, *1–7.*

Lichter, M., Vafeidis, A.T., Nicholls, R. J., & Kaiser, G. (2010). Exploring data related uncertainties in analyses of land area and population in the low elevation coastal zone (LECZ). *Coastal Res.*, *6*, 757–768.

Nkwunanwo, U. C., Malcolm W., & Brain, B. (2015). Flooding and flood risk reduction in Nigeria. *Cardinal gaps J. Geogr. Nat. Disasters*, *5*, 136.

Ritter, J., Berenguer, M., Corral, C., Park, S., & Sempere-Torres, D. (2020). Real-time assessment of flash flood impacts: A regional high-resolution method. *Environment International*, *136*, 105375.

Sofia, G., Roder, G., Dalla-Fontana, G., & Tarolli, P. (2017). Flood dynamics in urbanized landscapes: 100 years of climate and human's interaction. *Sci. Rep.*, *7*, 40527.

Suyeon, S., Sung-Ik, S., & Woonjae, H. (2018). Vortex simulations of Kelvin-Helmholtz instability with surface tension in density-stratified flows. *European Journal of Mechanics-B/Fluids*, *67*, 168-177.

Tomczyk, A. M., Ewertowski, M. W., & Carrivick, J. L. (2020). Geomorphological impacts of a glacier lake outburst flood in the high arctic Zackenberg River NE Greenland. *Journal of Hydrology*, *591*, 125300.

Viganò, D., & Maddalena, L. (2018). A numerical model for supersonic vortex dynamics. In *22nd AIAA International Space Planes and Hypersonics Systems and Technologies Conference* (p. 5162).

Wei, C., Haoyuan, H., Shaojun, L., Himan, S., Yi, W., Xiaojing, W., & Baharin, B. A. (2019). Flood susceptibility modelling using novel hybrid approach of reduced-error pruning trees with bagging and random subspace ensembles. *Journal of Hydrology*, *575*, 864–873.

Zeynab, S., Mehdi, D., & Hossein, H. Z. (2018). Numerical solution of 2D Navier – Stokes equation discretized via boundary elements method and finite difference approximation. *Engineering Analysis with Boundary Elements*, *96*, 64–77.